Supporting Information

Terbium-Fluorido Cluster: An Energy Cage for Photoluminescence

Bo-Kai Ling,[a] Junhao Li,[b] Yuan-Qi Zhai,[a] Hung-Kai Hsu,[c] Yi-Tsu Chan,[c] Wei-Peng Chen,[a] Tian Han[a] and Yan-Zhen Zheng*,[a]

Content

1. Materials and Measurements

All reagents and solvents for the syntheses were purchased from commercial sources and used as received. In particular, TbF_3 (99.9%) was obtained from ACMEC biochemical. $[Ln_2(O_2C^tBu)_6(HO_2C^tBu)_6]$ (Ln = Tb and Gd) were prepared as described previously.[S1] Elemental analyses (C, H and N) were performed on a Vario EL III elemental analyzer. The X-ray photoelectron spectroscopy (XPS) was measured on a Thermo Fisher ESCALAB Xi+ with Al monochromatic Al Kα excitation source. Matrix-assisted laser desorption/ionization coupled with a time-of-flight detector (MALDI-TOF) mass spectrometry was conducted on a Bruker autoflex™ speed MALDI/TOF mass spectrometer with a 355 nm frequency tripled Nd: YAG SmartBeam® laser. 1 μL of trans-2-[3-(4-tert-butyl-phenyl)-2-methyl-2-propenylidene] malono-nitrile (DCTB) solution (20 mg/mL in CH_3OH) was deposited on a MALDI plate and air-dried. Aliquots of a sample solution (100 μg/mL in CH_3OH) were added onto the matrix spots for the measurements acquired in linear mode. Infrared spectrum (4000-500 cm^{-1}) was recorded on a Thermo Scientific Nicolet 6700 FT-IR spectrophotometer. Solid state absorption UV-vis spectra were measured by a PE Lambda 950 UV-Vis-NIR spectrophotometer. Raman spectrum was performed on a Horiba LabRAM HR Evolution Laser Raman Spectrometer at room temperature. TGA experiments was carried out in a flow of nitrogen using a TGA-2 (METTLER TOLEDO) with a heating rate of 10 ℃/min. The compound is sensitive to loss of lattice solvent molecules when isolated from the mother-liquor. The particle size of TbF_3 (around 387 nm) was measured on a Zetasizer Nano ZSE granulometer. Room temperature luminescence spectra and decay curves were obtained on Edinburgh FLS980 Spectrometer. Low temperature luminescence spectra at 80 K and 4.2 K were measured at Wuhan National High Magnetic Center.

2. Synthesis

Synthesis of **1**. In a 30 mL scintillation vial, $Tb_2(piv)_6(Hpiv)_6$ (700 mg, 0.45 mmol) and NH_4F (74 mg, 2 mmol) are dissolved in 8 mL DMF. After 10 min ultrasonication, the vial was sealed and heated at 120 ℃ for 72 h. The solution was then cooled to room temperature and filtered. The filtrate was further cooled to -5 °C. After two days, colorless rod crystals suitable for X-ray single-crystal analysis are obtained (yield ~ 70 % based on Tb). Elemental analyses for $C_{85}H_{175}Tb_6F_8N_5O_{38}$, calculated: C, 34.25, H 5.92, N, 2.35; found: C, 33.29, H 5.65, N 2.40.

Table S1. Reported Ln-F clusters

Ln-F clusters	Ln	Ref
$[Yb_4(\mu\text{-}F)_4(Me_5C_5)_6]$	Yb	S2
$[Yb_5(\mu_4\text{-}F)(\mu_3\text{-}F)_2(\mu\text{-}F)_6(Me_5C_5)_6]$	Yb	S3
$[Sm_3(\mu\text{-}F)_3(\eta^5\text{-}C_5H_4{}^tBu)_6]$	Sm	S4
$[Yb_3(\mu\text{-}F)_3(\eta^5\text{-}C_5H_5)_6]$	Yb	S5
$[Yb_4(\mu\text{-}F)_4(Me_5C_5)_8]$	Yb	S5
$[Gd_4(\mu\text{-}F)_7(15\text{-crown-}5)_4][AsF_6]_5 \cdot 6SO_2$	Gd	S6
$[Er_3(OAr^{OMe})_4(\mu\text{-}F)_3(\mu_3\text{-}F)_2(thf)_4]\ thf \cdot 0.5C_6H_{14}$[a]	Er	S7
$[Ln_{28}(\mu\text{-}F)_{30}(\mu_3\text{-}F)_{20}(\mu_4\text{-}F)_{18}(SePh)_{16}(pyridine)_{24}]$	Nd, Pr	S8
$[Yb_4(\mu\text{-}F)_6(L)_6]$[b]	Yb	S9
$[Ln_3(\mu\text{-}F)_3(p\text{-}HC_6F_4N(CH_2)_2NMe_2)_6]$	La, Nd, Sm	S10, S11
$[Tb_6(\mu_3\text{-}F)_8(piv)_{10}(Hpiv)_4DMF]$	Tb	This work

[a] Ar^{OMe} = C_6H_2-2,6-Bu^t-4-OMe. [b] L = p-$HC_6F_4N(CH_2)_2NR_2$, R = Et or Me.

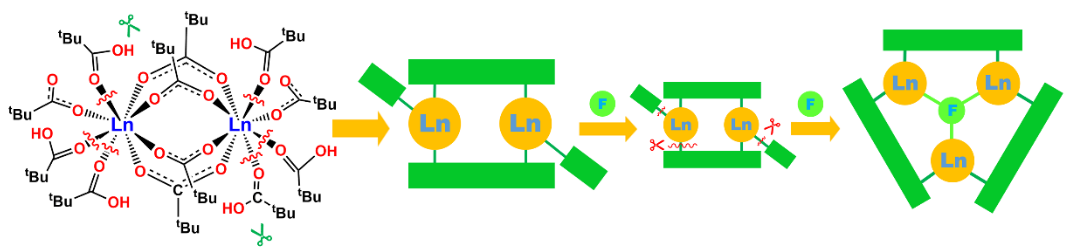

Fig. S1. Assumption of reaction process. The rectangle means the pivalate ligand. The yellow and lime circles are lanthanide and fluoride ions. Sticks in this Figure refer to chemical bonds.

3. Crystallography

Single-crystal X-ray diffraction data were collected on a Bruker Apex II DUO diffractometer at 150 K. The structure was solved by direct methods and all non-H atoms were subjected to anisotropic refinement by full-matrix least-squares refinement on *F2* using SHELXTL. The guest DMF molecules and guest water molecules in **1** are confirmed according to the TGA, elemental analyses. The CCDC deposition numbers for structures in this work are 1575579 (**1**). These data can be obtained free of charge via www.ccdc.cam.ac.uk/data_request/cif.

Table S2. Crystal data and structure refinement for **1**

Compound	**1**
Formula	$C_{85}H_{175}Tb_6F_8N_5O_{38}$
Formula weight	2980.87
Temperature / K	150.0
Crystal system	tetragonal
Space group	*P*nma
a/Å	36.191(9)
b/Å	23.761(9)
c/Å	15.011(4)
α/ °	90
β/ °	90
γ/ °	90
V/Å^3	12908(6)
Z	4
ρ_{calc} / g cm^{-3}	1.335
μ/mm^{-1}	3.306
GOF[a]	1.092
R_1, wR_2 [$I > 2\sigma(I)$] [b]	0.0980, 0.2307
R_1, wR_2 (all data)	0.1386, 0.2646

[a] $GOF = [\Sigma w(F_o^2 - F_c^2)^2/(n_{obc} - n_{param})]^{1/2}$.

[b] $R_1 = ||F_o| - |F_c||/\Sigma|F_o|$, $wR_2 = [\Sigma w(F_o^2 - F_c^2)^2/\Sigma w(Fo^2)^2]^{1/2}$.

4. Analysis of fluoride in 1

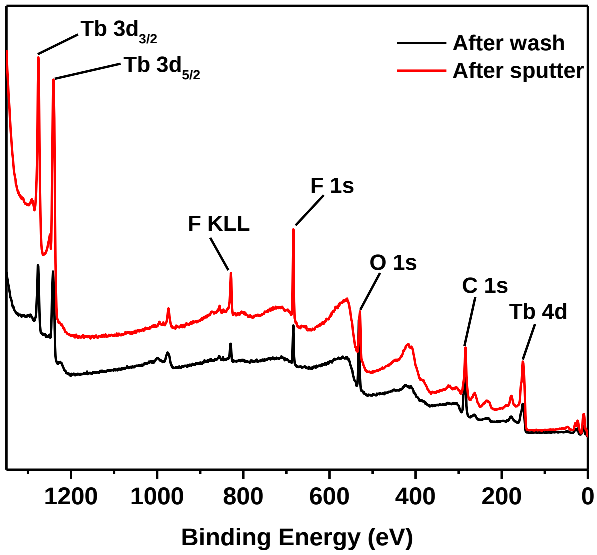

Fig. S2. XPS spectrum for complex **1**. The beam energy for in situ Ar ionic sputter was 3000 eV. On the surface of fresh **1** sample, the detected binding energies of Tb $3d_{3/2}$, Tb $3d_{5/2}$, Tb 4d, C 1s and O 1s locate at 1276, 1241, 151, 284 and 529 eV. The obvious F 1s and KLL peaks are observed at 684 and 829 eV, respectively, giving a strong evidence for the fluorido-bridges.

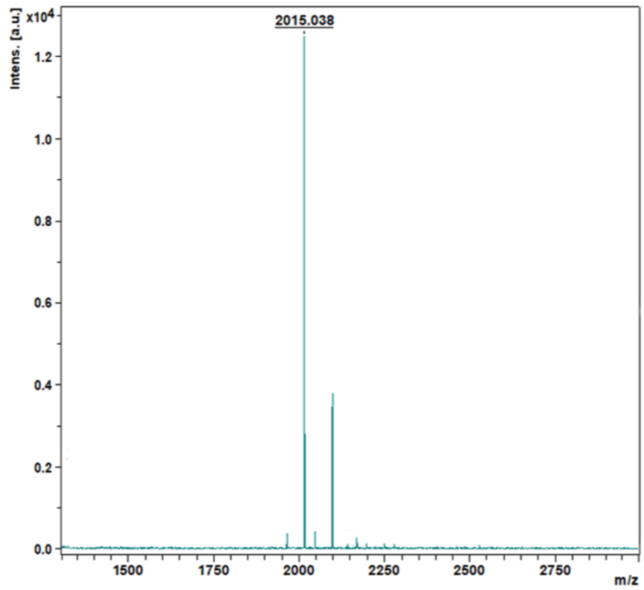

Fig. S3. The high resolution MALDI-TOF mass spectrum of complex **1** in CH_3OH solution in positive mode. The dominant peak for **1** locates at 2015.038. This corresponds to a reasonable formula of $[Tb_6F_8(piv)_9]^+$ (calcd. Mw = 2015.082).

5. TGA Curve for Complex 1

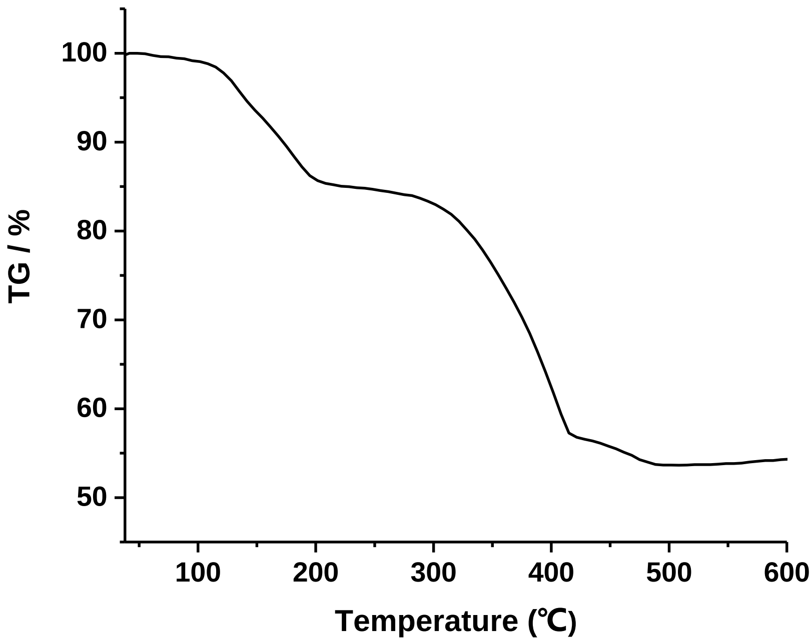

Fig. S4. TGA curve for complex **1**. Thermogravimetric analysis (TGA) indicates a weight loss of 12.8 % from room temperature to 195 °C, corresponding to the removal of the lattice guests (H_2O and DMF, *calcd* 12.8%). A plateau region is observed from 195 to 300 ℃, indicating the high thermostability of the cluster.

6. Structural Details for Complex 1

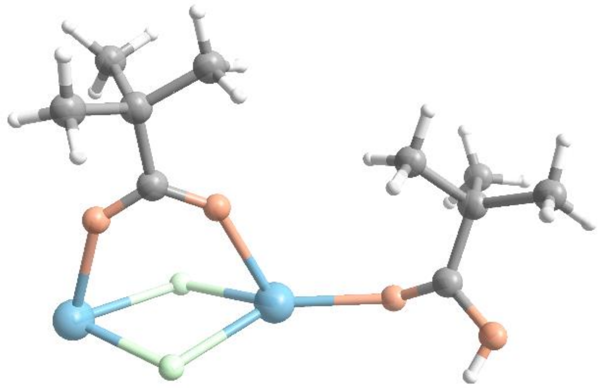

Fig. S5. Coordination mode of complex **1**.

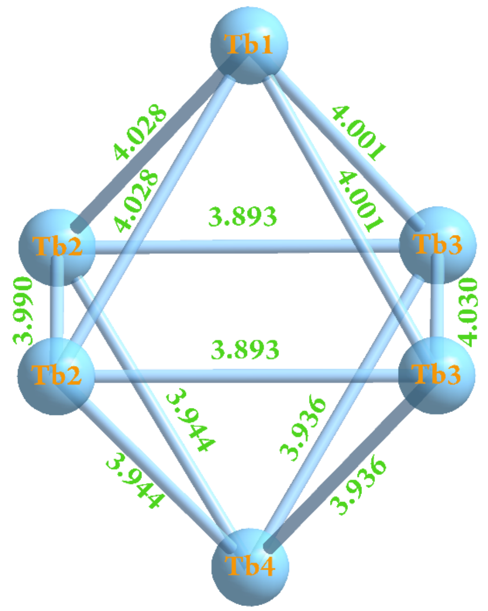

Fig. S6. Distances between Tb ions in complex **1** cluster.

7. Absorption spectra for pivalate ligand.

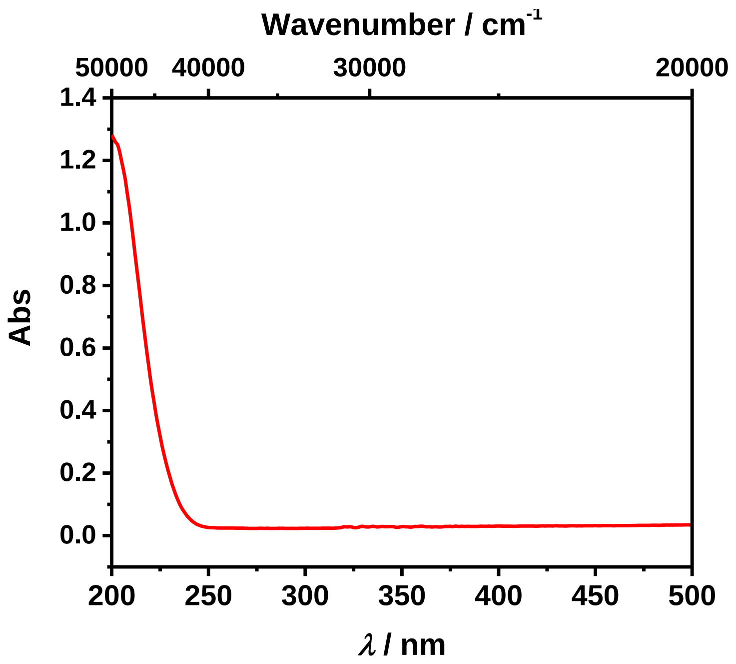

Fig. S7. Absorption spectrum of sodium pivalate.

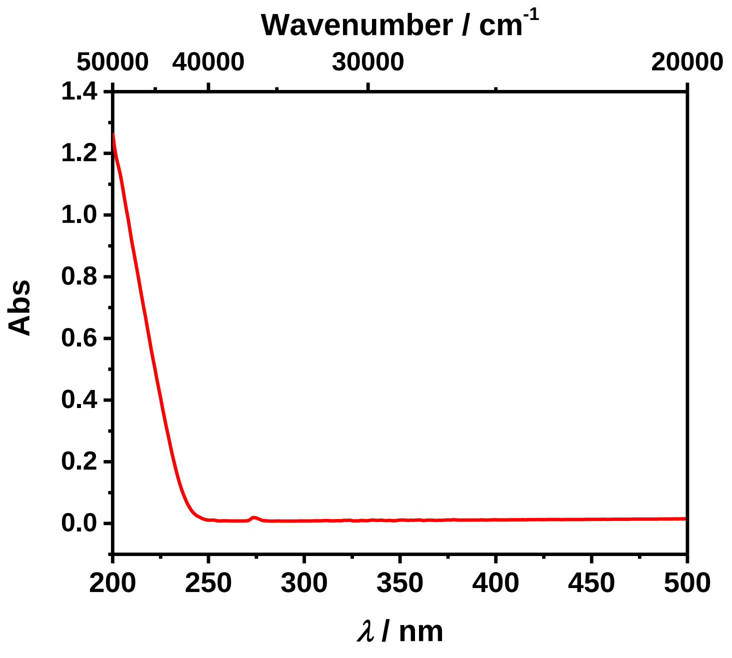

Fig. S8. Absorption spectrum of $[Gd_2(O_2C^tBu)_6(HO_2C^tBu)_6]$. As shown in Figs. S7 and S8, the energy position of the singlet state (S1) of pivalate ligand was determined from the edge of the absorption spectra, which corresponds to an energy of 40000 cm^{-1} (250 nm).

8. Luminescence Supplements

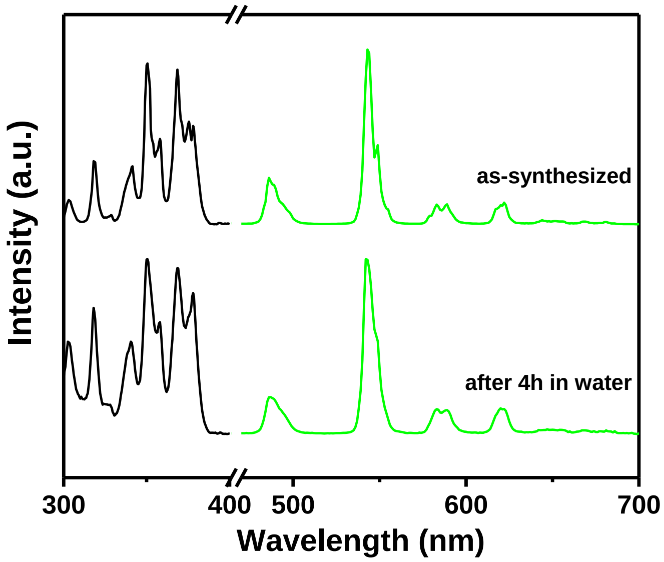

Fig. S9. Luminescence spectra of complex **1** collected during water stability test.

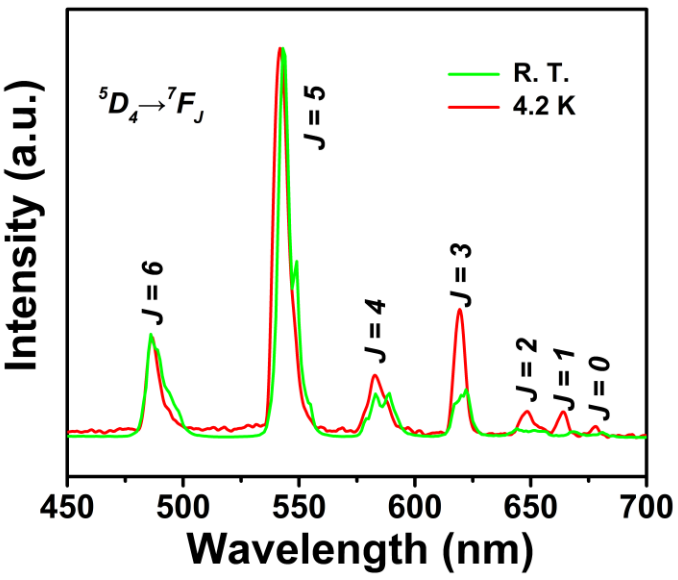

Fig. S10. Emission spectra for complex **1** at room temperature and 4.2 K. The wavelength of excitation light is 350 nm and the emission spectra are normalized.

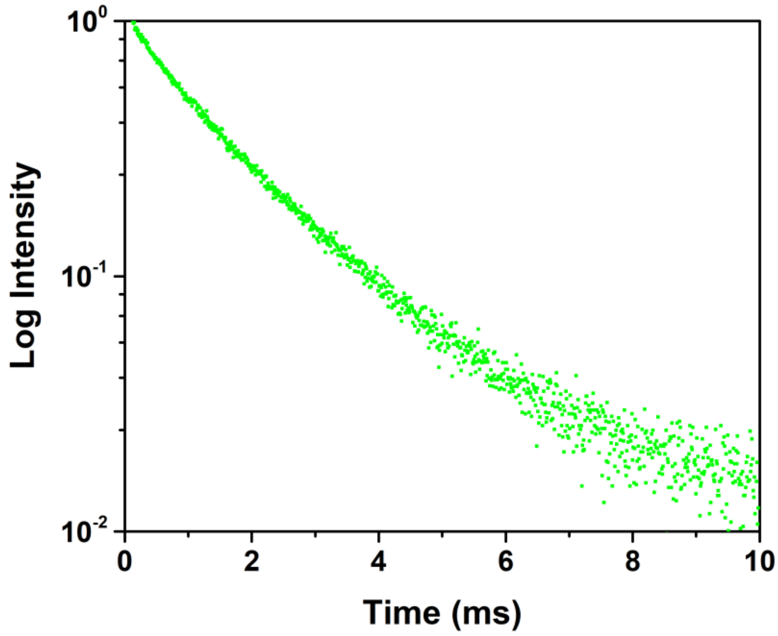

Fig. S11. The decay curve for TbF_3 nanoparticles. The curve is fitted with the first order exponential equation and the value of lifetime is 1.43 ms. This value is close to reported value of TbF_3 crystals.[S12]

8. Colour Purity

The difference on color purities between **1** and terbium fluoride nanomaterial, the color purities for them at room temperature were calculated using:[S13]

$$Colour\ \ purity = \frac{\sqrt{(\mathrm{x_s} - \mathrm{x_i})^2 + (\mathrm{y_s} - \mathrm{y_i})^2}}{\sqrt{(x_d - \mathrm{x_i})^2 + (y_d - \mathrm{y_i})^2}} \times 100\%$$

In this equation, (x_d, y_d) is the coordinate of the Tb^{3+} ion dominant wavelength, (x_s, y_s) is the coordinate of sample point, and (x_i, y_i) is the coordinate of the illuminant point (0.310, 0.316). Here, the dominant emission wavelengths for TbF_3 and **1** are 543 nm and the CIE coordinates for them are (0.366, 0.545) and (0.312, 0.574), respectively (Fig. S12). The calculated result shows that color purity for **1** (60.8%) is higher than that for TbF_3 (55.4%).

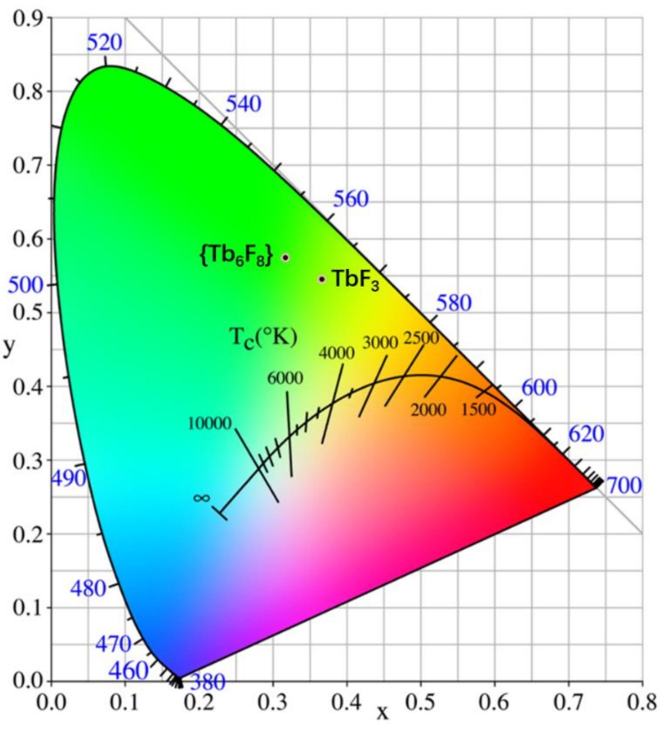

Fig. S12. The CIE chromaticity coordinates for complex **1** and TbF_3. As shown, the emission color for complex **1** is greener than TbF_3.

9. Quantum Yield

Solid quantum yields were measured by an Edinburgh FLS980 with integrating sphere and Hamamatsu C9920 absolute photoluminescence quantum yield measurement system. Since the maximal light absorption for complex **1** cluster is about 20%, when different amounts of samples were added in the powder tray (FLS980) and quartz vessel (C9920), absorption of contamination and holder will affect the quantum yield measurement. So we used a brand-new reference blanking plug as the sample holder. (Caution! It is very dangerous to use the reference plug as sample holder and very easy to damage the integrating sphere). The solid quantum yield of **1** was measured for several times in different batches of samples. Each time, the excitation wavelength was set to be 350 nm with the integral ranging from 340 nm to 360 nm, and the emission ranging from 450 nm to 700 nm was recorded. In order to obtain the accurate quantum yield, each peak of Tb^{3+} was integrated separately. The quantum yields have no significant change and 99.6(2)% is finally determined. Meanwhile, we also used the Hamamatsu C9920 absolute photoluminescence quantum yield measurement system with the same integration method to determine the quantum yield of **1**, which gives 100% quantum yield. After soaking complex **1** in water for 4 hours, it still exhibits nearly the same photoluminescence and excitation (PL and PLE) spectra as before (Fig. S9 in SI), indicating that the luminescence of **1** is stable in the water. Meanwhile, the quantum yield of this sample after is also tested and the value of 80.3% is determined. Compound **1** is not stable in neither acidic nor alkaline environments since the luminescence of **1** in 1M HCL, 0.01M HCl, 1M NaOH and 0.01M NaOH aqueous solution are all quenched. The quantum yield for TbF_3 was determined by Hamamatsu C9920 absolute photoluminescence quantum yield measurement system. For TbF_3, the excitation wavelength was set to be 350 nm with the integral ranging from 340 nm to 360 nm. And the emission ranging from 450 nm to 700 nm was recorded. The quantum yield for TbF_3 is determined to be 15.0(2)% under 350 nm UV-light. The accuracy of Edinburgh FLS980 with integrating sphere was determined by Rhodamine B and Rhodamine 6G standard sample from Edinburgh company (Table S3). The accuracy of Hamamatsu quantum yield system was determined by diluted fluorescein and anthracene solution (Table S4).

Table S3. References for quantum yields in Edinburgh FLS980 with integrating sphere

Standard Sample	λex (nm)	QY (tested)	QY (standard)	Solvent	Abs
Rhodamine B	514	29.8%	31 %	water	0.01
Rhodamine 6G	488	93.7%	91 %	ethanol	0.01

Table S4. References for quantum yields in Hamamatsu quantum yield system

Standard Sample	QY (tested)	QY (literature value)	Solvent	Conc. [M]	Reference
Anthracene	27.6%	28%	ethanol	1.0×10^{-6}	S13
Fluorescein	88.9%	88%	0.1N NaOH	1.0×10^{-5}	S14

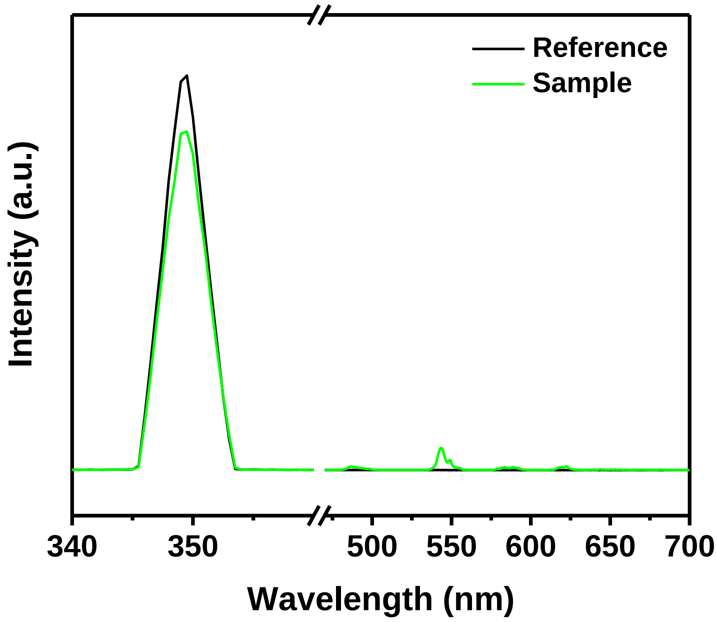

Fig. S13. Left part: the excitation intensity provided by light source (black) and rest of excitation intensity that goes through the measured complex **1** (green). Right part: the emission intensity of reference (black) and complex **1** recorded by an integrating sphere.

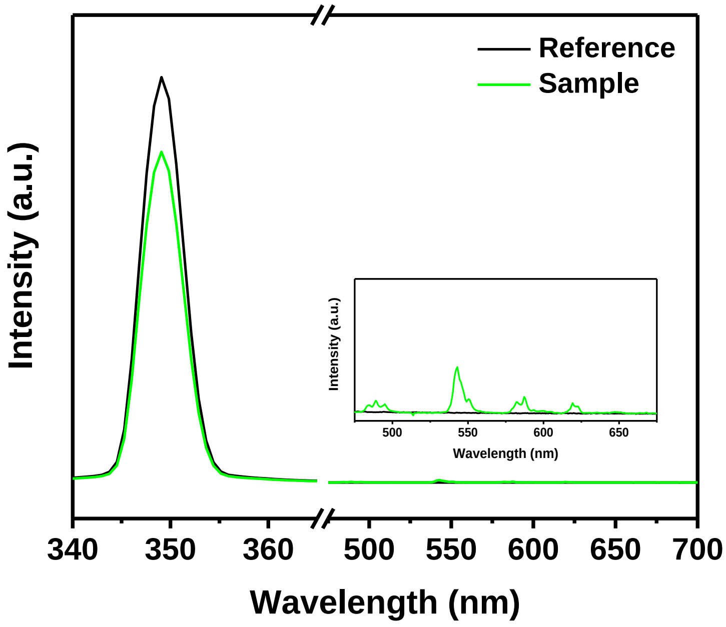

Fig. S14. Left part: the excitation intensity provided by light source (black) and rest of excitation intensity that goes through the measured TbF_3 (green). Right part: the emission intensity of reference (black) and TbF_3 recorded by an integrating sphere.

10. Probability of Energy Migration

On the basis of single crystal diffraction, the average distance between two Tb ions within the cluster is 3.968 Å and that between two clusters is 11.062 Å. Due to the long distance between Tb ions, we considered that the electric exchange interaction in **1** is negligible.[S15] Thus, the energy migration in **1** can be governed by dipole–dipole (d–d), dipole–quadrupole (d–q) or quadrupole–quadrupole (q–q) interactions, in which the probability P is proportional to r^{-6}, r^{-8} and r^{-10}, respectively (where r is the average Tb–Tb distance).[S16-S18] According to this, we conclude that the probability of energy migration within intra-cluster (P_{intra}) is about 469–28315 times higher than that of inter-cluster energy migration (P_{inter}). The large ratio suggests that the energy migration between the clusters can be neglected.

11. DFT Calculation Details

Geometry optimisations of model 1 and model 2 were performed in the gas-phase with DFT using the Gaussian 09 (rev. D) software package.[S19] In order to facilitate SCF convergence, the gadolinium atoms were exchanged for yttrium. The PBE density functional was used in conjunction with Grimme's D3 dispersion correction.[S20-S24] The cc-pVDZ basis set was used for the carbon and hydrogen atoms and the cc-pVTZ basis set was used for the fluorine and oxygen atoms.[S25,S26] For yttrium the Stuttgart RSC 1997 effective core potential (ECP) was employed for the 28 core electrons, and the remaining valence electrons were described with the corresponding valence basis set. [S27-S29] In order to obtain the correct harmonic vibrational modes, the atomic mass of yttrium was set to 158.92 (the natural abundance-weighted mass of terbium).

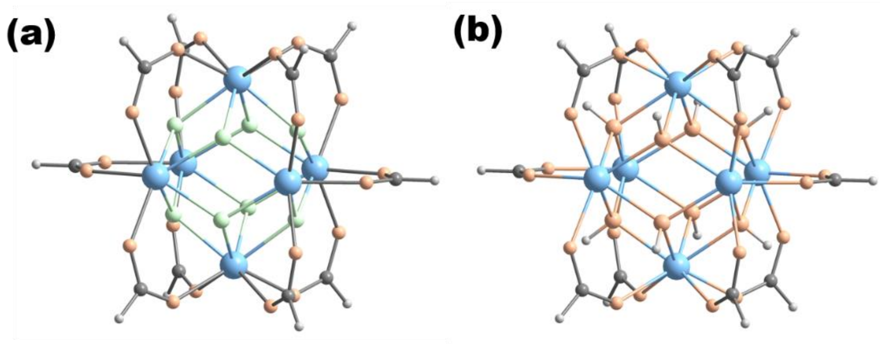

Fig. S15. The optimized structure of **model 1** (a) and **model 2** (b). Color codes: Tb, skyblue; F, beige; O, light salmon; C, grey; H, light grey.

Table S5. The optimized structure of model 1.

Atom label	x	y	z
Y(Iso=158.92)	0.82174	-2.50957	1.3E-5
Y(Iso=158.92)	-1.82314	-0.59685	-1.80687
Y(Iso=158.92)	1.82314	0.59683	-1.80685
Y(Iso=158.92)	1.82314	0.59686	1.80685
Y(Iso=158.92)	-1.82314	-0.59681	1.80684
F	0.36581	-1.11776	-1.74439
F	2.08418	-0.65074	8E-6
F	-1.29577	-1.75769	-1E-6
F	0.3658	-1.11773	1.74439
O	-0.22831	-3.85641	-1.49793
O	2.46961	-2.97684	-1.49356
O	2.46966	-2.97682	1.49355
O	-0.22825	-3.85636	1.49804
Y(Iso=158.92)	-0.82175	2.50959	-1.1E-5
F	-0.36579	1.11772	-1.7444
F	1.29576	1.75773	-1E-5
O	1.69682	2.55289	-2.84748
O	3.85675	1.26683	-1.18314
O	2.88062	-1.05633	-2.84196
F	-0.3658	1.11776	1.7444
F	-2.08417	0.65074	-2.7E-5
O	0.22826	3.85639	1.49798
O	-2.4696	2.97675	1.49359
O	-2.46963	2.97682	-1.49358
O	0.22825	3.85636	-1.49804
O	3.85676	1.26683	1.18313
O	2.88057	-1.0563	2.84197
O	1.69682	2.55293	2.84745
O	-1.69676	-2.5529	-2.84749
O	-2.88065	1.05629	-2.84196
O	-3.85676	-1.26684	-1.18315
O	-3.85674	-1.26688	1.18313
O	-1.69675	-2.55283	2.84751
O	-2.88074	1.05627	2.84199
C	-1.04996	-3.66965	-2.50797
C	3.02474	-2.33816	-2.50049
C	3.02473	-2.33813	2.50051
C	-1.04991	-3.66957	2.50807
C	1.05001	3.66963	-2.50799
C	4.41767	1.45453	-8E-6

C	1.05002	3.66967	2.50795
C	-3.0248	2.3381	2.5005
C	-3.02481	2.33811	-2.50047
C	-4.41765	-1.45458	-8E-6
H	-5.49299	-1.81381	-4E-6
H	5.49303	1.81373	-1.1E-5
H	3.71959	-2.94246	3.16408
H	-1.24495	-4.56619	-3.17622
H	-1.24487	-4.56608	3.17637
H	3.7196	-2.94251	-3.16405
H	1.24507	4.56624	3.17614
H	-3.71968	2.94247	3.16401
H	-3.71974	2.94243	-3.16397
H	1.24507	4.56619	-3.17619

Table S6. The optimized structure of model 2.

Atom label	x	y	z
Y(Iso=158.92)	-8.27E-4	2.65619	-1.15E-4
Y(Iso=158.92)	1.97593	4.55E-4	-1.8325
Y(Iso=158.92)	-1.97589	-7.38E-4	-1.83256
Y(Iso=158.92)	-1.97594	-4.56E-4	1.83253
Y(Iso=158.92)	1.97585	7E-4	1.83252
O	1.43864	3.65044	-1.50872
O	-1.44093	3.64957	-1.50874
O	-1.44094	3.64972	1.50834
O	1.4387	3.6506	1.5083
Y(Iso=158.92)	8.28E-4	-2.65618	9.8E-5
O	-2.53909	-1.96	-2.80587
O	-4.15259	-0.00149	-1.19206
O	-2.54009	1.95807	-2.80609
O	-1.43865	-3.6504	1.50872
O	1.44092	-3.64953	1.50868
O	1.441	-3.64972	-1.50829
O	-1.43861	-3.65055	-1.50839
O	-4.15263	-9.84E-4	1.19202
O	-2.54017	1.95842	2.80594
O	-2.539	-1.95967	2.80599
O	2.53884	1.95965	-2.80604
O	2.54045	-1.95846	-2.80571
O	4.15263	0.00131	-1.19202
O	4.15256	0.00132	1.1921
O	2.53894	1.95995	2.80586

O	2.54017	-1.9581	2.80606
C	2.25098	3.21367	-2.45323
C	-2.25301	3.21228	-2.45326
C	-2.25293	3.21257	2.45298
C	2.25102	3.21394	2.45291
C	-2.25105	-3.21395	-2.45291
C	-4.73048	-0.00142	-2.8E-5
C	-2.2511	-3.21367	2.45315
C	2.25302	-3.21229	2.4532
C	2.2532	-3.21259	-2.45277
C	4.73048	0.00154	5.4E-5
H	5.86594	0.00197	8.4E-5
H	-5.86595	-0.00177	-4.7E-5
H	-2.78411	4.01398	3.05846
H	2.78175	4.01531	-3.05876
H	2.78172	4.01566	3.05839
H	-2.78429	4.01359	-3.05877
H	-2.78193	-4.01532	3.0586
H	2.7843	-4.01363	3.05868
H	2.78451	-4.01401	-3.05813
H	-2.7818	-4.01571	-3.05831
O	-1.91312	-1.35444	5.8E-5
O	-1.91408	1.3534	-1.05E-4
O	-3.73E-4	1.22945	-1.91807
O	4.19E-4	-1.22982	-1.91826
O	-3.9E-4	1.22976	1.91813
O	3.24E-4	-1.22953	1.91822
O	1.91404	-1.35337	1E-4
O	1.91318	1.3545	-7.6E-5
H	5.96E-4	-1.94905	2.63264
H	-2.71536	-1.97073	1.07E-4
H	-2.71674	1.96913	-1.1E-4
H	6.55E-4	-1.94951	-2.63251
H	-7.07E-4	1.94936	2.63248
H	2.71544	1.97076	-6.9E-5
H	2.71666	-1.96916	1.62E-4
H	-5.61E-4	1.94891	-2.63255

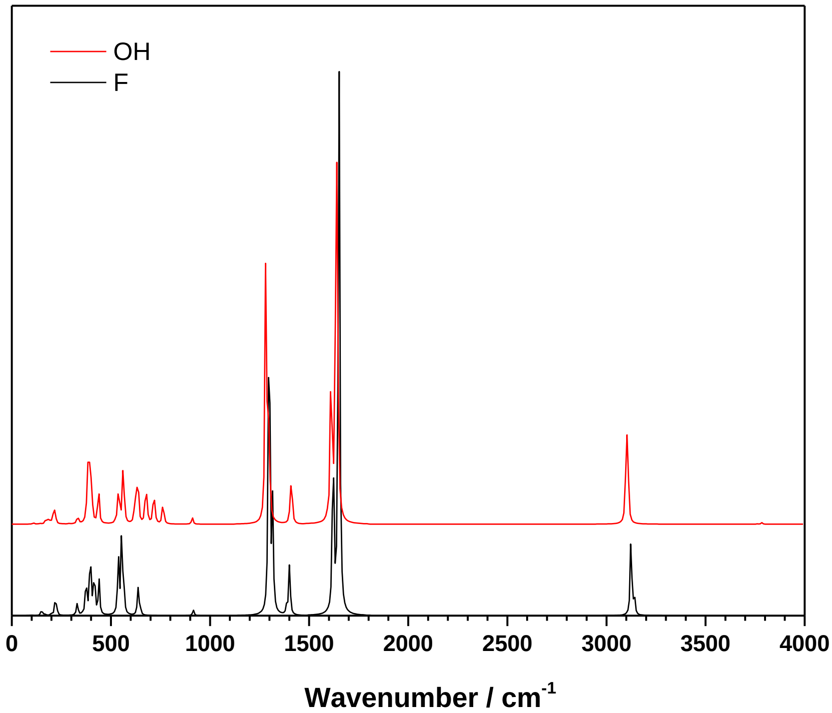

Fig. S16. The calculated IR Spectrum of **model 1** and **model 2** in the region 0 – 4000 cm^{-1}. Black line represents the calculated spectrum for **model 1** while red line represents the calculated spectrum for **model 2.**

Table S7: Calculated vibrational mode energies from IR spectrum for model 1.

Frequency / cm^{-1}	Intensity	Frequency / cm^{-1}	Intensity	Frequency / cm^{-1}	Intensity
0	0.07652	700	3.32495	1456	8.54567
7	0.09463	707	2.78816	1463	5.97018
14	0.10602	714	2.38246	1470	5.40594
21	0.12265	721	1.36203	1477	4.17869
28	0.14002	728	1.01486	1484	4.032
35	0.16167	735	0.86572	1491	6.79933
42	0.2088	742	0.7511	1498	9.84937
49	0.24841	749	0.65785	1505	10.57782
56	0.3055	756	0.62198	1512	11.49309
63	0.56795	763	0.57309	1519	12.62606
70	0.82988	770	0.52456	1526	14.02235
77	1.06819	777	0.48496	1533	15.74735
84	1.64425	784	0.45294	1540	17.89467
91	4.77364	791	0.42757	1547	20.53461
98	5.63013	798	0.18622	1554	24.00642
105	6.38869	805	0.19064	1561	28.3897
112	2.6294	812	0.12197	1568	34.26541

119	2.42963	819	0.14026	1575	42.89887
126	3.20348	826	0.163	1582	55.75848
133	5.41843	833	0.19176	1589	77.50045
140	13.42934	840	0.22884	1596	115.45715
147	51.72617	847	0.2778	1603	179.99872
154	47.82523	854	0.34432	1610	378.20511
161	23.15675	861	0.43788	1617	1389.85157
168	19.14802	868	0.5754	1624	1806.79038
175	11.91091	875	0.78928	1631	686.52894
182	8.14097	882	1.14833	1638	911.02341
189	9.89163	889	1.81979	1645	3007.60326
196	23.60223	896	3.29995	1652	7136.12969
203	34.0661	903	7.60748	1659	1739.24468
210	42.16615	910	28.51744	1666	578.49407
217	170.80368	917	70.52589	1673	283.18605
224	154.64704	924	15.34122	1680	168.0622
231	62.90823	931	5.19579	1687	111.52404
238	21.76684	938	2.53316	1694	79.56108
245	10.82341	945	1.48829	1701	59.70397
252	7.1847	952	0.97667	1708	46.50627
259	5.99539	959	0.68934	1715	37.2789
266	5.34595	966	0.51222	1722	30.56819
273	5.24635	973	0.39546	1729	25.53148
280	6.2708	980	0.31447	1736	21.65246
287	6.50285	987	0.25602	1743	18.60013
294	7.10825	994	0.21246	1750	16.15423
301	8.69746	1001	0.17913	1757	14.15836
308	11.82855	1008	0.15307	1764	12.51641
315	19.40277	1015	0.13231	1771	11.1457
322	48.49332	1022	0.1155	1778	9.98942
329	158.07754	1029	0.1017	1785	7.49603
336	78.13371	1036	0.09023	1792	6.77169
343	34.55438	1043	0.0806	1799	6.14747
350	35.28058	1050	0.07243	1806	5.60573
357	57.54012	1057	0.06544	1813	1.3161E-6
364	89.41416	1064	0.05942	2968	0.77323
371	318.76045	1071	0.05419	2975	0.8475
378	362.7463	1134	0.00127	2982	1.0885
385	195.55484	1141	3.24266	2989	1.20228
392	547.68746	1148	3.55171	2996	1.33491
399	640.43778	1155	3.90712	3003	1.4908
406	261.24996	1162	5.25647	3010	1.67573
413	431.92209	1169	5.8279	3017	1.89741

420	390.10557	1176	6.49807	3024	2.16627
427	140.42021	1183	7.29115	3031	2.49675
434	199.08204	1190	8.23925	3038	2.90927
441	481.85709	1197	9.38568	3045	3.43349
448	115.65989	1204	10.79005	3052	4.11383
455	48.10028	1211	12.53626	3059	5.01929
462	29.50835	1218	14.74544	3066	6.26172
469	22.14494	1225	17.59775	3073	8.03248
476	19.09774	1232	21.44133	3080	10.68139
483	18.14922	1239	26.58785	3087	14.90512
490	18.67109	1246	34.33379	3094	22.26001
497	20.88265	1253	45.13074	3101	36.83285
504	25.54996	1260	62.07975	3108	72.33055
511	34.63171	1267	90.99694	3115	197.65878
518	54.00394	1274	146.68136	3122	939.70502
525	106.6838	1281	276.49252	3129	492.9576
532	344.72029	1288	701.08398	3136	218.92303
539	772.61236	1295	3122.67318	3143	239.7636
546	355.84445	1302	2788.32808	3150	66.57263
553	1046.88337	1309	946.79053	3157	31.26768
560	584.73224	1316	1636.213	3164	18.80044
567	371.18892	1323	483.9623	3171	12.73196
574	113.85852	1330	188.30686	3178	9.25218
581	54.42881	1337	105.73079	3185	7.04976
588	34.19323	1344	70.57733	3192	5.55971
595	25.13026	1351	52.59644	3199	4.50148
602	20.78743	1358	43.07928	3206	3.7215
609	20.27508	1365	39.33435	3213	3.12937
616	24.30577	1372	42.31578	3220	2.66891
623	39.86253	1379	63.02832	3227	2.30357
630	112.15836	1386	163.98814	3234	2.00873
637	370.15403	1393	179.40957	3241	1.76728
644	171.2404	1400	665.29075	3248	1.56703
651	94.49653	1407	253.39636	3255	1.39907
658	30.62187	1414	75.77669	3262	1.2568
665	15.99497	1421	37.32014	3269	1.13523
672	10.32144	1428	23.33986	3276	1.03051
679	7.43582	1435	16.59352	3283	0.93967
686	5.72512	1442	12.72918	3290	0.17626
693	4.60614	1449	10.25655	3297	0.16082

Table S8: Calculated vibrational mode energies from IR spectrum for model 2.

Frequency / cm^{-1}	Intensity	Frequency / cm^{-1}	Intensity	Frequency / cm^{-1}	Intensity
0	0.03516	800	6.20546	1640	4745.18989
8	0.04063	808	4.60729	1648	1661.64243
16	0.08472	816	3.6263	1656	465.3119
24	0.11922	824	2.9815	1664	216.14275
32	0.16994	832	2.54196	1672	125.65495
40	0.22128	840	2.01245	1680	82.55031
48	0.26044	848	1.68982	1688	58.55811
56	0.48724	856	1.62587	1696	43.78574
64	0.62882	864	1.66794	1704	34.02272
72	0.77777	872	1.86663	1712	27.22274
80	1.05375	880	2.04043	1720	22.29089
88	1.61201	888	3.29542	1728	18.59692
96	2.79224	896	7.05801	1736	15.7566
104	8.79957	904	26.58197	1744	13.52453
112	14.26706	912	81.26733	1752	11.7083
120	4.84875	920	15.91327	1760	10.25818
128	3.56654	928	4.96759	1768	9.06293
136	6.31862	936	2.36875	1776	6.55209
144	9.59324	944	1.37734	1784	5.84842
152	7.674	952	0.89856	1792	5.25233
160	12.64337	960	0.63182	1800	2.37963
168	46.14234	968	0.46826	2944	1.02987
176	54.56632	976	0.36083	2952	1.4017
184	63.53729	984	0.28652	2960	1.56302
192	51.77241	992	0.233	2968	1.75389
200	52.45384	1000	0.19317	2976	1.982
208	134.26869	1008	0.16275	2984	2.25772
216	184.30852	1016	0.13898	2992	2.59527
224	72.25954	1024	0.12006	3000	3.01464
232	20.86833	1032	0.10476	3008	3.54461
240	11.00691	1040	0.09221	3016	4.2278
248	7.50312	1048	0.08178	3024	5.12959
256	5.95494	1056	0.07303	3032	6.35433
264	5.29632	1064	0.06561	3040	8.07708
272	5.19155	1072	0.01298	3048	10.60996
280	6.25877	1120	3.91788E-5	3056	14.55453
288	10.0798	1128	2.95324	3064	21.19596
296	7.5635	1136	3.28499	3072	33.70056
304	8.52082	1144	4.5719	3080	61.71059

312	11.45396	1152	5.13769	3088	146.84522
320	19.97224	1160	5.81561	3096	625.01466
328	64.58607	1168	6.63744	3104	1170.6159
336	77.53291	1176	7.6471	3112	549.64906
344	31.19801	1184	8.90667	3120	130.3378
352	31.49802	1192	10.50623	3128	54.85791
360	47.61341	1200	12.5806	3136	30.49841
368	92.4899	1208	15.3389	3144	19.48178
376	277.69825	1216	19.12002	3152	13.53897
384	811.49208	1224	24.50305	3160	9.96145
392	811.52229	1232	32.54588	3168	7.63874
400	612.21335	1240	45.35518	3176	6.04459
408	254.74814	1248	67.703	3184	4.90281
416	93.72274	1256	112.40078	3192	4.05688
424	82.97054	1264	220.81527	3200	3.41263
432	221.237	1272	616.07104	3208	2.91064
440	397.20801	1280	3420.33878	3216	2.51187
448	81.05611	1288	1609.862	3224	2.18983
456	35.3205	1296	1374.16001	3232	1.92601
464	22.28301	1304	569.95348	3240	1.70718
472	17.20884	1312	181.95924	3248	1.52364
480	15.32846	1320	93.59445	3256	1.3682
488	14.94294	1328	58.79428	3264	0.27588
496	16.12266	1336	41.33915	3608	0.00316
504	19.7116	1344	31.48505	3616	0.00351
512	28.64664	1352	25.68947	3624	0.01622
520	61.23571	1360	22.5099	3632	0.01806
528	121.00558	1368	21.51296	3640	0.02022
536	397.39623	1376	23.16834	3648	0.0228
544	287.71122	1384	29.85493	3656	0.02591
552	186.79146	1392	52.04152	3664	0.02971
560	703.35383	1400	164.59636	3672	0.03442
568	368.50614	1408	503.12947	3680	0.04037
576	100.04848	1416	316.38856	3688	0.04803
584	48.40014	1424	73.95606	3696	0.05813
592	36.26903	1432	32.52323	3704	0.0719
600	37.71576	1440	19.03379	3712	0.09139
608	58.12501	1448	10.3895	3720	0.12047
616	169.76456	1456	9.01431	3728	0.16718
624	349.52975	1464	6.59296	3736	0.25115
632	482.71907	1472	5.70054	3744	0.43494
640	418.68545	1480	7.83237	3752	1.04087
648	101.43171	1488	10.39787	3760	4.71967

656	61.78444	1496	11.02659	3768	2.45608
664	82.1582	1504	11.95982	3776	4.68336
672	304.31457	1512	13.22989	3784	19.33285
680	391.10615	1520	14.90445	3792	3.59449
688	127.4732	1528	17.09612	3800	1.12902
696	59.7042	1536	19.98391	3808	0.53962
704	72.45908	1544	23.85513	3816	0.3156
712	258.65601	1552	29.18936	3824	0.20723
720	314.04327	1560	36.84209	3832	0.14662
728	88.16064	1568	48.45608	3840	0.10928
736	39.48189	1576	67.7624	3848	0.08463
744	30.9935	1584	111.08373	3856	0.0675
752	50.2134	1592	201.75298	3864	0.05511
760	221.40973	1600	383.44591	3872	0.04585
768	148.72063	1608	1737.02039	3880	0.03875
776	35.67881	1616	1269.61418	3888	0.03319
784	16.10819	1624	796.44271	3896	0.02874
792	9.45625	1632	2596.71208	3904	0.02514

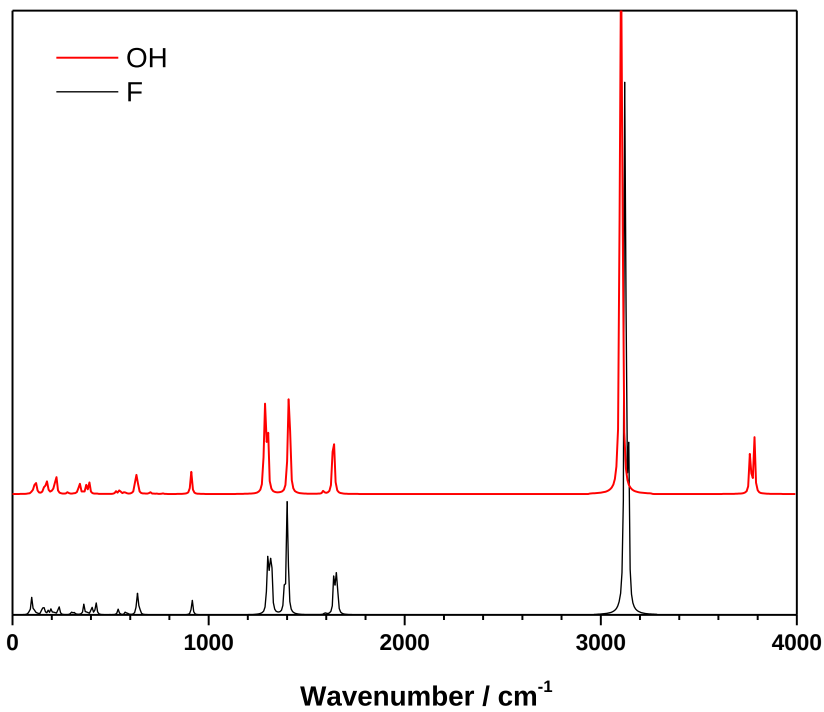

Fig. S17. The calculated Raman Spectrum of **model 1** and **model 2** in the region 0 – 4000 cm^{-1}. Black line represents the calculated spectrum for **model 1** while red line represents the calculated spectrum for **model 2.**

Table S9: Calculated vibrational mode energies from Raman spectrum for model 1.

Frequency / cm^{-1}	Intensity	Frequency / cm^{-1}	Intensity	Frequency / cm^{-1}	Intensity
0	0.00398	700	0.01107	1463	0.0602
7	0.00482	707	0.00885	1470	0.04625
14	0.00559	714	0.00729	1477	0.03868
21	0.00657	721	0.00612	1484	0.03169
28	0.00806	728	0.00521	1491	0.02773
35	0.00979	735	0.00449	1498	0.02734
42	0.01251	742	0.00374	1505	0.02527
49	0.01602	749	0.00324	1512	0.0238
56	0.02157	756	0.00316	1519	0.02286
63	0.03083	763	0.00345	1526	0.02238
70	0.04919	770	0.00327	1533	0.02237
77	0.10019	777	0.00315	1540	0.02285
84	0.26587	784	0.00307	1547	0.02278
91	0.47269	791	0.00304	1554	0.02462
98	1.44344	798	0.00194	1561	0.02507
105	0.54916	805	0.0021	1568	0.02552
112	0.39815	812	0.00195	1575	0.03373
119	0.22753	819	0.00224	1582	0.05246
126	0.16711	826	0.0026	1589	0.12344
133	0.10679	833	0.00306	1596	0.16727
140	0.12738	840	0.00364	1603	0.12195
147	0.36187	847	0.00442	1610	0.117
154	0.57309	854	0.00547	1617	0.16925
161	0.60417	861	0.00694	1624	0.30354
168	0.2502	868	0.00911	1631	0.74465
175	0.17316	875	0.01246	1638	3.22598
182	0.39035	882	0.01806	1645	2.45933
189	0.20861	889	0.02846	1652	3.48978
196	0.49692	896	0.05115	1659	1.8685
203	0.24338	903	0.11596	1666	0.52028
210	0.22016	910	0.42081	1673	0.23822
217	0.19246	917	1.19544	1680	0.13763
224	0.14791	924	0.26632	1687	0.09013
231	0.39579	931	0.08766	1694	0.06381
238	0.65607	938	0.04215	1701	0.04764
245	0.18079	945	0.02457	1708	0.03696
252	0.06735	952	0.01604	1715	0.02954

259	0.03811	959	0.01129	1722	0.02416
266	0.02804	966	0.00837	1729	0.02014
273	0.02523	973	0.00645	1736	0.01705
280	0.02716	980	0.00512	1743	0.01462
287	0.0385	987	0.00416	1750	0.01264
294	0.09249	994	0.00345	1757	0.01104
301	0.22875	1001	0.00291	1764	0.0097
308	0.17905	1008	0.00248	1771	0.00862
315	0.19767	1015	0.00214	1778	0.00772
322	0.08209	1022	0.00187	1785	0.00695
329	0.06486	1029	0.00165	1792	0.00629
336	0.04419	1036	0.00146	1799	0.00572
343	0.05992	1043	0.0013	1806	0.0028
350	0.09675	1050	0.00117	1813	0.00256
357	0.22936	1057	0.00106	2968	0.03729
364	0.89202	1064	9.60562E-4	2975	0.04087
371	0.27557	1071	8.75833E-4	2982	0.05436
378	0.23877	1141	6.64603E-4	2989	0.06002
385	0.18123	1148	0.00459	2996	0.06661
392	0.14018	1155	0.00504	3003	0.07435
399	0.37603	1162	0.00984	3010	0.08352
406	0.61862	1169	0.01084	3017	0.09451
413	0.22504	1176	0.01201	3024	0.10783
420	0.39938	1183	0.01337	3031	0.12418
427	0.98136	1190	0.01498	3038	0.14457
434	0.24929	1197	0.0169	3045	0.17044
441	0.09261	1204	0.01922	3052	0.20397
448	0.04633	1211	0.02205	3059	0.24851
455	0.02918	1218	0.02556	3066	0.30951
462	0.02083	1225	0.03	3073	0.39625
469	0.01616	1232	0.0369	3080	0.52563
476	0.01387	1239	0.04456	3087	0.73123
483	0.01348	1246	0.06221	3094	1.08773
490	0.01424	1253	0.07754	3101	1.79038
497	0.01947	1260	0.09997	3108	3.4906
504	0.01857	1267	0.13505	3115	9.44601
511	0.01915	1274	0.19547	3122	44.07503
518	0.02644	1281	0.3169	3129	25.35167
525	0.0472	1288	0.64445	3136	11.74991
532	0.13909	1295	1.94078	3143	14.27597
539	0.47638	1302	4.84906	3150	3.77429
546	0.15142	1309	3.67847	3157	1.70544
553	0.05674	1316	4.68034	3164	1.00443

560	0.04365	1323	3.89704	3171	0.67185
567	0.06415	1330	1.01387	3178	0.48427
574	0.22436	1337	0.47468	3185	0.36689
581	0.16428	1344	0.30567	3192	0.28812
588	0.12724	1351	0.24399	3199	0.23252
595	0.05636	1358	0.23413	3206	0.19174
602	0.04514	1365	0.27014	3213	0.16089
609	0.05546	1372	0.38723	3220	0.13698
616	0.08784	1379	0.78609	3227	0.11806
623	0.18377	1386	2.48834	3234	0.10282
630	0.62432	1393	2.57612	3241	0.09037
637	1.78183	1400	9.37138	3248	0.08005
644	0.77768	1407	4.03248	3255	0.07141
651	0.41043	1414	1.09427	3262	0.06411
658	0.12865	1421	0.48847	3269	0.05787
665	0.06351	1428	0.27803	3276	0.0525
672	0.03845	1435	0.1811	3283	0.04785
679	0.026	1442	0.12835	3290	0.01066
686	0.01884	1449	0.09631	3297	0.00973
693	0.01433	1456	0.0751		

Table S10: Calculated vibrational mode energies from Raman spectrum for model 2.

Frequency / cm^{-1}	Intensity	Frequency / cm^{-1}	Intensity	Frequency / cm^{-1}	Intensity
0	0.00235	800	0.00391	1640	4.11565
8	0.0032	808	0.00398	1648	0.98063
16	0.00436	816	0.0043	1656	0.30579
24	0.00521	824	0.00484	1664	0.14706
32	0.00617	832	0.00564	1672	0.08648
40	0.00752	840	0.00678	1680	0.05699
48	0.00943	848	0.00843	1688	0.04042
56	0.01223	856	0.01089	1696	0.03017
64	0.01787	864	0.01461	1704	0.02339
72	0.02888	872	0.02103	1712	0.01867
80	0.04584	880	0.03293	1720	0.01525
88	0.06342	888	0.05874	1728	0.0127
96	0.18306	896	0.13227	1736	0.01073
104	0.3556	904	0.48961	1744	0.00919
112	0.74607	912	1.84067	1752	0.00781
120	0.91141	920	0.36457	1760	0.00682
128	0.28951	928	0.11125	1768	0.00601
136	0.12183	936	0.05212	1776	0.00534

144	0.1125	944	0.03001	1784	0.00477
152	0.1968	952	0.01945	1792	0.00429
160	0.56538	960	0.01362	1800	0.00225
168	0.7033	968	0.01006	2944	0.03793
176	1.04743	976	0.00774	2952	0.05225
184	0.34371	984	0.00613	2960	0.05826
192	0.19801	992	0.00498	2968	0.06536
200	0.27864	1000	0.00412	2976	0.07384
208	0.45291	1008	0.00347	2984	0.08409
216	0.91043	1016	0.00296	2992	0.09663
224	1.39661	1024	0.00256	3000	0.11221
232	0.30442	1032	0.00223	3008	0.13189
240	0.10955	1040	0.00196	3016	0.15723
248	0.06075	1048	0.00174	3024	0.19067
256	0.0427	1056	0.00155	3032	0.23604
264	0.03705	1064	0.00139	3040	0.29979
272	0.04618	1072	3.90311E-4	3048	0.3934
280	0.14774	1120	2.2355E-4	3056	0.53896
288	0.08097	1128	0.00509	3064	0.78354
296	0.03705	1136	0.00564	3072	1.24279
304	0.03598	1144	0.01116	3080	2.26772
312	0.06438	1152	0.01247	3088	5.36757
320	0.07012	1160	0.01402	3096	22.66725
328	0.1682	1168	0.01588	3104	44.85827
336	0.48613	1176	0.01815	3112	21.94941
344	0.84441	1184	0.02094	3120	5.12088
352	0.21499	1192	0.02442	3128	2.11344
360	0.2098	1200	0.02887	3136	1.16486
368	0.20814	1208	0.03465	3144	0.74056
376	0.76739	1216	0.04239	3152	0.51312
384	0.38902	1224	0.05307	3160	0.37676
392	0.96203	1232	0.06844	3168	0.28848
400	0.19383	1240	0.09175	3176	0.22802
408	0.0696	1248	0.13085	3184	0.18478
416	0.04129	1256	0.20787	3192	0.15279
424	0.03406	1264	0.35753	3200	0.12845
432	0.03619	1272	0.80565	3208	0.1095
440	0.01623	1280	3.02846	3216	0.09446
448	0.01147	1288	7.48071	3224	0.08232
456	0.00941	1296	4.31329	3232	0.07238
464	0.00831	1304	5.07003	3240	0.06414
472	0.00914	1312	1.0723	3248	0.05723
480	0.0097	1320	0.45276	3256	0.05138

488	0.01058	1328	0.26485	3264	0.0109
496	0.01231	1336	0.18697	3608	0.00287
504	0.01618	1344	0.15181	3616	0.00319
512	0.02786	1352	0.13943	3624	0.00646
520	0.07588	1360	0.14428	3632	0.00722
528	0.23756	1368	0.16882	3640	0.00813
536	0.11232	1376	0.22624	3648	0.00922
544	0.30535	1384	0.35943	3656	0.01055
552	0.20295	1392	0.74914	3664	0.0122
560	0.07378	1400	2.69884	3672	0.01427
568	0.14978	1408	7.84623	3680	0.01691
576	0.12681	1416	5.2077	3688	0.02038
584	0.05709	1424	1.14343	3696	0.02506
592	0.04317	1432	0.46916	3704	0.0316
600	0.05431	1440	0.25548	3712	0.04116
608	0.09434	1448	0.15722	3720	0.05599
616	0.21446	1456	0.10834	3728	0.08104
624	0.93688	1464	0.07498	3736	0.12898
632	1.5878	1472	0.05692	3744	0.24192
640	0.88845	1480	0.04672	3752	0.63786
648	0.2091	1488	0.04081	3760	3.32528
656	0.08727	1496	0.03509	3768	1.70787
664	0.05028	1504	0.03106	3776	1.32933
672	0.04811	1512	0.02827	3784	4.70189
680	0.03587	1520	0.02649	3792	0.93293
688	0.03196	1528	0.0256	3800	0.30707
696	0.07492	1536	0.02558	3808	0.15328
704	0.15108	1544	0.02657	3816	0.09282
712	0.03604	1552	0.02895	3824	0.06264
720	0.0342	1560	0.03373	3832	0.04529
728	0.02919	1568	0.04331	3840	0.03435
736	0.03244	1576	0.07061	3848	0.02699
744	0.0153	1584	0.26156	3856	0.02179
752	0.01221	1592	0.1416	3864	0.01797
760	0.02679	1600	0.09873	3872	0.01508
768	0.0494	1608	0.1375	3880	0.01284
776	0.01359	1616	0.25984	3888	0.01107
784	0.00739	1624	0.73923	3896	0.00964
792	0.00466	1632	3.49671	3904	0.00848

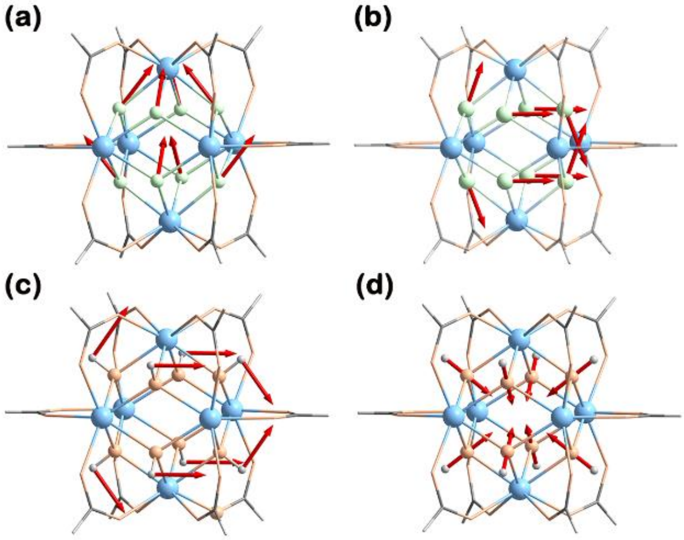

Fig. S18. Corresponding energy frequencies for F^- ions are 537 cm^{-1} (a) and 555 cm^{-1} (b); for OH^- ions are 716 cm^{-1} (c), 3762 and 3783 cm^{-1} (d). Each arrowhead represents vibration direction of F^- or OH^- ions. Color codes: Tb, skyblue; F, beige; O, light salmon; C, grey; H, light grey.

12. IR and Raman Spectra for Complex 1

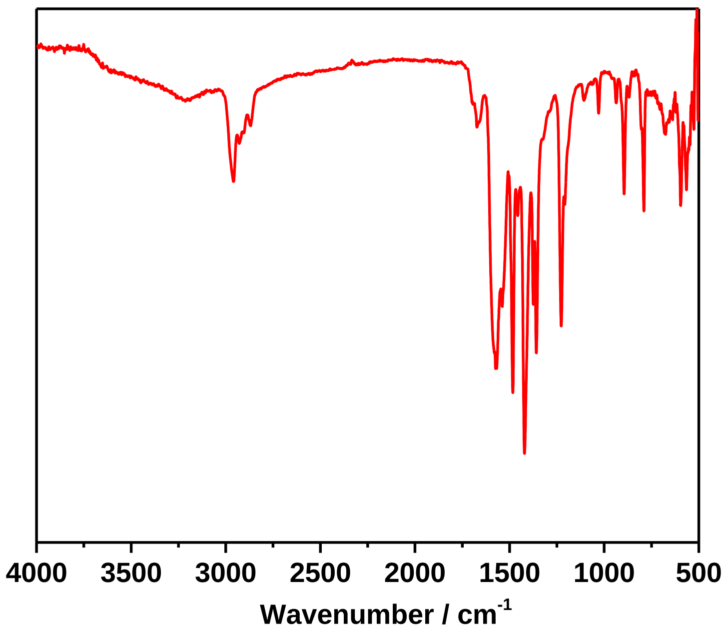

Fig. S19. IR spectrum for complex **1**

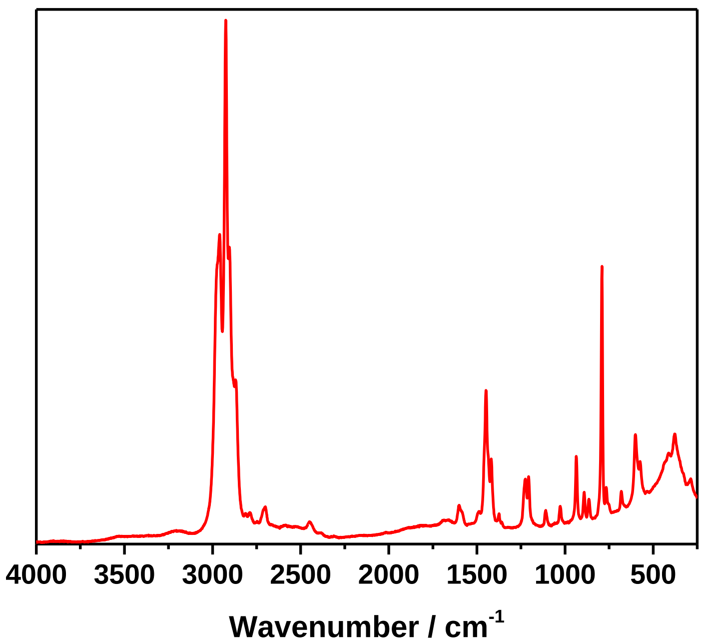

Fig. S20. Raman spectrum for complex **1** under 532 nm laser.

13. Selected Bond Lengths and Angles for Complex 1

Table S11. Selected bond lengths [Å] for **1**

Tb1—Tb3	4.0008 (15)	Tb3—Tb3*	4.0302 (12)
Tb2—Tb2*	3.9905 (19)	Tb4—Tb2	3.9436 (14)
Tb2—Tb1	4.0440 (10)	Tb4—Tb3	3.9358 (15)
Tb2—Tb3	3.8930 (16)		
Tb1—F3	2.349 (9)	Tb1—F4	2.519 (14)
Tb1—F6	2.513 (12)	Tb2—F1	2.337 (9)
Tb2—F2	2.363 (7)	Tb2—F3	2.354 (10)
Tb2—F4	2.384 (7)	Tb3—F1	2.325 (10)
Tb3—F3	2.324 (10)	Tb3—F5	2.388 (7)
Tb3—F6	2.390 (7)	Tb4—F1	2.311 (9)
Tb4—F2	2.462 (12)	Tb4—F5	2.459 (14)
Tb1—O8	2.348 (15)	Tb1—O10	2.362 (13)
Tb1—O12	2.503 (19)	Tb2—O1	2.271 (17)
Tb2—O5	2.354 (12)	Tb2—O7	2.320 (13)
Tb2—O9	2.358 (12)	Tb3—O2	2.320 (14)
Tb3—O3	2.360 (12)	Tb3—O11	2.346 (13)
Tb3—O16	2.393 (18)	Tb4—O4	2.372 (12)
Tb4—O6	2.308 (9)		

Symmetry code: (*) *x*, −*y*+3/2, *z*.

Table S12. Selected angles [deg] for **1**

Tb1—F3—Tb2	117.9 (4)	Tb1—F4—Tb2	110.5 (4)
Tb1—F3—Tb3	117.8 (4)	Tb1—F6—Tb3	109.4 (3)
Tb2—F2—Tb2*	115.2 (5)	Tb2—F4—Tb2*	113.7 (5)
Tb2—F1—Tb3	113.2 (4)	Tb2—F3—Tb3	112.7 (4)
Tb2—F1—Tb4	116.1 (4)	Tb2—F2—Tb4	109.6 (3)
Tb3—F5—Tb3*	115.1 (5)	Tb3—F6—Tb3*	115.0 (5)
Tb3—F1—Tb4	116.2 (4)	Tb3—F5—Tb4	108.6 (4)

Symmetry code: (*) *x*, −*y*+3/2, *z*.

14. Reference

S1. Y. Z. Zheng, M. Evangelisti and R. E. Winpenny, *Angew. Chem. Int. Ed.*, 2011, **50**, 3692-3695.

S2. C. J. Burns, D. J. Berg and R. A. Andersen, *J. Chem. Soc., Chem. Commum.*, 1987, 272-273.

S3. P. L. Watson, T. H. Tulip and I. Williams, *Organometallics*, 1990, **9**, 1999-2009.

S4. H. Schumann, M. R. Keitsch, J. Winterfeld and J. Demtschuk, *J. Organomet. Chem.*, 1996, **525**, 279-281.

S5. B. D. Glen, M. Gerd and S. Dirk, *Eur. J. Inorg. Chem.*, 2000, 1061-1071.

S6. G. B. Deacon, et al. *Dalton Trans.*, 2005, 2237-2238.

S7. G. B. *Dalton Trans.*, 2006, 802-812.

S8. M. Romanelli, G. A. Kumar, T. J. Emge, R. E. Riman and J. G. Brennan, *Angew. Chem. Int. Ed*., 2008, **47**, 6049-6051.

S9. G. B. Deacon, C. M. Forsyth, P. C. Junk and J. Wang, *Chem. Eur., J.* 2009, **15**, 3082-3092.

S10. G. B. Deacon, et al. *Dalton Trans*., 2012, **41**, 8624-8634.

S11. G. B. Deacon, P. C. Junk, R. P. Kelly and J. Wang, *Dalton Trans*., 2016, **45**, 1422-1435.

S12. V. I. Kushnirenko, M. V. Sopinskyy, E. G. Manoilov and V. S. Khomchenko, *J. Alloys Compd.*, 2008, **451**, 209-211.

S13. W. R. Dawson and M. W. Windsor, *J. Phys. Chem.*, 1968, 72, 3251-3260.

S14. D. F. Eaton, *Pure Appl. Chem.*, 1988, 60, 1107-1114.

S15. Y.-F. Wu, Y.-T. Nien, Y.-J. Wang, I.-G. Chen and J. McKittrick, *J. Am. Ceram. Soc*., 2012, **95**, 1360-1366.

S16. T. Főrster, *Discuss. Faraday Soc*., 1959, **27**, 7-17.

S17. D. L. Dexter, *J. Chem. Phys*., 1953, **21**, 836-850.

S18. O. L. Malta, *J. Non-Cryst. Sol*., 2008, **354**, 4770-4776.

S19. M. J. Frisch, et al. Gaussian 09, Revision A. 02. Gaussian, Inc., Wallingford CT. 2016.

S20. J. P. Perdew, K. Burke and M. Ernzerhof, *Phys. Rev. Lett*., 1996, **77**, 3865-3868.

S21. J. P. Perdew, K. Burke and M. Ernzerhof, *Phys. Rev. Lett*., 1997, **78**, 1396-1396.

S22. S. Grimme, *J. Comput. Chem*., 2006, **27**, 1787-1799.

S23. S. Grimme, *Wiley Interdiscip. Rev. Comput. Mol. Sci*., 2011, **1**, 211-228.

S24. S. Grimme, *J. Comput. Chem*., 2004, **25**, 1463-1473.

S25 D. E. Woon and T. H. Dunning, *J. Chem. Phys*., 1993, **98**, 1358-1371.

S26. T. H. Dunning, *J. Chem. Phys*., 1989, **90**, 1007-1023.

S27. M. Kaupp, P. v. R. Schleyer, H. Stoll and H. Preuss, *J. Chem. Phys*., 1991, **94**, 1360-1366.

S28. M. Dolg, H. Stoll, H. Preuss and R. M. Pitzer, *J. Phys. Chem*., 1993, **97**, 5852-5859.

S29. A. Bergner, M. Dolg, W. Küchle, H. Stoll and H. Preuß, *Mol. Phys*., 2006, **80**, 1431-1441.